Journal of Cleaner Production 545 (2026) 147741

Contents lists available at ScienceDirect

Journal of Cleaner Production

journal homepage: www.elsevier.com/locate/jclepro

Metal removal and valorization using *Dactylococcopsis salina* 16Som2: Insights into metal binding properties and catalytic activity of metal-enriched biomass

Matilde Ciani [a], Giovanni Orazio Lepore [b,*], Giorgio Facchetti [c], Karima Guehaz [a,d], Alessandro Puri [e,f], Raffaella Gandolfi [c], Isabella Rimoldi [c], Roberto De Philippis [a], Alessandra Adessi [a]

[a] Department of Agriculture, Food, Environment and Forestry (DAGRI), University of Florence, Florence, Italy
[b] Department of Earth Sciences (DST), University of Florence, Florence, Italy
[c] Department of Pharmaceutical Sciences (DISFARM), University of Milan, Milan, Italy
[d] Laboratory for the Protection of Ecosystems in Arid and Semi-Arid Zones, FNSV, Kasdi Merbah University, Ouargla, Algeria
[e] Department of Physics and Astronomy, Alma Mater Studiorum – University of Bologna, Bologna, Italy
[f] CNR-IOM-OGG c/o ESRF – the European Synchrotron, Grenoble, France

HIGHLIGHTS

- Cyanobacteria can efficiently remove heavy metals from contaminated waters.
- Cyanobacteria have potential as green catalysts in pharmaceutical applications.
- Their dual-purpose application reflects circular economy principles.
- A detailed atomistic characterization of metal-organic interaction is provided.

GRAPHICAL ABSTRACT

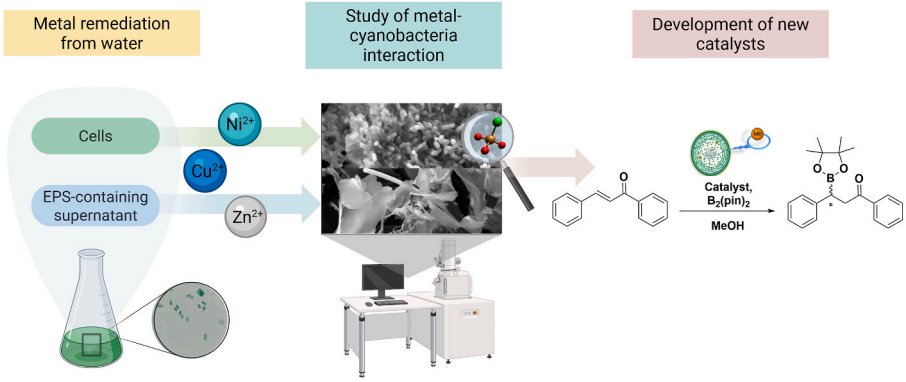

ARTICLE INFO

Keywords:
Binding properties
Bioremediation
Catalytic activity
Circular economy
Cyanobacteria
EXAFS
Metal biosorption

ABSTRACT

This study explores the dual potential of the cyanobacterium *Dactylococcopsis salina* for heavy metal removal and its application as a sustainable catalyst. Focusing on the biosorption of Cu(II), Ni(II), and Zn(II), we employed advanced analytical techniques, including SEM-EDX, FT-IR, and X-ray absorption spectroscopy, to elucidate the metal-binding patterns in both cellular and soluble fractions of the cyanobacterium. Cu(II) exhibits the highest biosorption affinity, accumulating in the cellular and soluble fractions at 3.7% and 7.0% (w/w), respectively. Our findings reveal distinct binding preferences for each metal ion, with coordination modes predominantly involving mixed (O,N)-(Cl,S) ligands. The (O,N):(Cl,S) ratio varied significantly based on the metal type, the biosorbent fraction, and the presence of multiple metals, with a ratio close to 0.5 and 0.75 for Cu(II) (fourfold

* Corresponding author.
E-mail address: giovanniorazio.lepore@unifi.it (G.O. Lepore).

https://doi.org/10.1016/j.jclepro.2026.147741
Received 23 January 2025; Received in revised form 20 January 2026; Accepted 4 February 2026
Available online 9 February 2026

coordinated) in the soluble and cellular fraction, respectively; a ratio close to 0.5, that decreases to 0 when more than one metal is present in the solution for Zn(II) (fourfold coordinated) in both fractions; and a ratio of 1 for Ni (II) (exclusively bonded to O/N in sixfold coordination). The type of biosorbed metal plays a critical role in the determination of catalytic performances: in borylation reactions of α,β-unsaturated chalcones with bis(pinacolato)diboron, Cu(II)- and multimetal-enriched biosorbents demonstrated outstanding catalytic activity (up to 94% conversion efficiency), whereas Zn(II)-enriched samples delivered modest performance. This study thus establishes a direct link between metal-binding chemistry of cyanobacteria-based biosorbents and catalytic functionality, paving the way for tailored catalyst design.

By integrating metal remediation and catalyst development, these results contribute to the advancement of cleaner production strategies through resource recovery and waste valorization.

1. Introduction

In the face of escalating environmental challenges, finding sustainable solutions for environmental remediation and resource recovery has never been more pressing. Developing innovative strategies to address pollution, coupled with the efficient use of resources, including waste valorization, is essential for creating a more sustainable future. These strategies are at the core of cleaner production, which aims to minimize waste and environmental impact while maximizing resource efficiency. Cyanobacteria, photoautotrophic prokaryotic microorganisms, have emerged as promising bioremediation and resource recovery platforms, including metal biosorption and valorization sectors (Ciani and Adessi, 2023). Beyond their recognized efficiency in bioremediation and heavy metal removal, cyanobacteria are increasingly valued for a wide range of biotechnological applications. These microorganisms serve as sustainable platforms for soil restoration, the production of biofuels, pigments (such as phycobiliproteins), and high-value bioactive compounds with antioxidant, anti-inflammatory, and antimicrobial properties (Do Nascimento et al., 2019; Franco-Morgado et al., 2023; Ren et al., 2025). This versatility makes cyanobacteria key components in the transition toward a circular economy, where biological waste is transformed into valuable resources (Ren et al., 2025).

The ability of cyanobacteria to remove metals is driven mainly by the production of exopolysaccharides (EPS) (Mota et al., 2022) that surround the cells through more or less condensed fractions and can be partly released in the medium (Rossi and De Philippis, 2016). EPS provide functional groups such as hydroxyl, carboxyl, sulfate, amino groups, and uronic acids that contribute to the binding of metal ions (Kumawat et al., 2021; Momin et al., 2024). Other mechanisms underlying metal removal by cyanobacteria primarily involve surface adsorption, complexation, ion exchange, and precipitation (De Philippis et al., 2011; Priya et al., 2022; Ramesh et al., 2023). These interactions result in the sequestration of metals from the surrounding environment, often facilitating their immobilization into the biomass. The binding of metals to cyanobacterial EPS has been associated with different processes, such as electrostatic interactions, coordination bonds, and/or van der Waals interactions, all of which can contribute to the biosorption capacity (Momin et al., 2024; Yadav et al., 2021). In addition to EPS, cyanobacteria synthesize different metal-binding proteins that can be found inside or outside the cell, such as metallothioneins — small molecular weight proteins rich in cysteinyl residues with the primary function of metal storage and transportation — which bind to the metal ions through cysteinyl thiolate bridges (Chakdar et al., 2022; Yadav et al., 2021). These proteins are usually associated with Zn(II) and Cu(II) but also bind with other toxic metals such as Cd(II), Hg (II), and Pb(II) (Chakdar et al., 2022; Yadav et al., 2021). Nevertheless, direct information regarding the chemical environment of the metals upon binding is missing.

A further issue commonly faced after metal biosorption is the management of polluted sludges: valorizing metal-loaded biomasses for applications such as catalysis, adsorption, chemical sensing, antibacterial materials, micronutrient fertilizers, and production of gases and biochar through pyrolysis has been proposed as an effective strategy to reduce the environmental impact of metal pollution while creating added-value products (Bădescu et al., 2018; Chai et al., 2022; Kirchon et al., 2018; Samoraj et al., 2019). Such valorization strategies offer a pathway toward cleaner production by transforming waste streams into valuable resources, reducing both environmental contamination and the demand for virgin materials (Diankristanti and Ng, 2024). Utilizing cyanobacteria in these processes could thus enhance the sustainability of industrial and municipal waste management by recovering metals for reuse and transforming the resulting biomass into bioproducts. For example, metal-enriched biomass can be used as a hybrid catalyst to develop more efficient and sustainable methods for synthesizing biologically active compounds—such as antioxidants or anti-inflammatory agents—and key pharmaceutical intermediates required for the manufacture of drugs. Indeed, transition metal-catalyzed reactions can accelerate otherwise challenging chemical transformations, ensuring high selectivity and yield. Transition metal complexes based on iridium (Chauhan et al., 2024; Facchetti and Rimoldi, 2018), ruthenium (Hafeez et al., 2022) and copper (Facchetti et al., 2023; Shilpa et al., 2021) are widely used to facilitate a broad range of chemical processes, contributing to the synthesis of enantiopure drug precursors or other biologically relevant compounds (Compagno et al., 2023; Rossino et al., 2022).

Green catalysts have the potential to catalyze different chemical reactions, being an essential alternative to environmentally unsafe chemical mechanisms (Kate et al., 2022). Moreover, this becomes even more impactful within a framework of circular economy that translates into finding ways to recycle or recover materials endowed with catalytic properties, thus reducing the need for virgin metal resources (Zanetti et al., 2022). In this case, the metal-organic complexes obtained by merging the chelating properties of cyanobacteria with the transition metals to be removed can be adopted as hybrid catalysts by directly exploiting and valorizing the metals bound to the surface of the cells without the need for further steps for desorption and/or recovery.

The integration of bioremediation with catalytic reuse of metals aligns with the principles of cleaner production by closing material loops and minimizing the environmental footprint of chemical manufacturing (Gandolfi et al., 2022; Murrieta et al., 2024). Specifically, the use of metals from wastewater as catalysts through cyanobacteria-mediated bioremediation exemplifies how innovation can align with environmental sustainability (Al-Amin et al., 2021).

While significant progress has been obtained in exploring the biosorption capabilities of cyanobacteria, their binding mechanisms are not fully understood and the application of metal-enriched cyanobacteria obtained after biosorption has never been studied. Addressing these gaps could yield valuable insights into the binding properties and chemical-structural characteristics of the newly formed metal-organic compounds as well as promote waste valorization, embracing a circular economy approach. Achieving precise control over metal binding in biomass would enable the optimization of the biosorption process and synthesis of customized materials with targeted functionalities, thereby opening new markets for these biologically derived products.

Hence, this study aims to investigate the innovative use of two types of cyanobacteria-based biosorbents, derived from (i) cellular and (ii) soluble fractions, for the removal and valorization of Cu(II), Ni(II), and Zn(II) from aqueous solutions, exploring the interaction between metals and cyanobacteria and the possible application of the metal-organic

materials obtained at the end of the process. Thus, the catalytic properties of the biosorbed metals in the addition of bis(pinacolato)diboron to α,β-unsaturated chalcones were evaluated after the optimization of reaction conditions. This particular substrate was chosen due to its innumerable uses, both as a building block for the synthesis of more complex molecules and for its therapeutic potential, which is mainly linked to its antioxidant activity (Iacovino et al., 2021; Mezgebe et al., 2023; WalyEldeen et al., 2023). The cyanobacterium selected for this study was the halophilic *Dactylococcopsis salina* 16Som2, which had already shown high EPS production and metal removal capabilities (Ciani et al., 2024). Given the heterogeneity of biological materials, the interaction between the metals and the biomass was studied adopting two separated fractions to verify a different role in metal biosorption and provide more accurate information regarding metal binding properties. Integrating different analytical techniques, such as Scanning Electron Microscopy with Energy Dispersive X-ray analysis (SEM-EDX), Fourier-transform infrared spectroscopy (FT-IR), X-ray absorption near edge structure (XANES) and Extended X-ray absorption fine structure (EXAFS) spectroscopy, can offer a comprehensive understanding of the interaction between metals and heterogeneous biological materials (Kassem et al., 2023). By characterizing the chemical and structural properties of the newly formed metal-organic materials generated during biosorption, we seek to unveil the binding mechanisms and their potential for high-value applications. By integrating high-resolution structural characterization of metal binding to different fractions with the first assessment of metal-loaded cyanobacterial biomass as a functional catalyst, this study aims to establish a new, direct link between cyanobacteria-mediated bioremediation and sustainable resource valorization, thereby offering a novel pathway for the development of tailored, bio-derived catalytic materials in a circular economy framework.

2. Materials and methods

2.1. Cyanobacterium growth and biosorbent preparation

Dactylococcopsis salina 16Som2 (Genbank: OQ945751) was selected for its ability to produce EPS and remove metals (Ciani et al., 2024) and grown in sea-water medium enriched as follows (g L^{-1}): $NaNO_3$, 1.5; Na_2HPO_4, 0.04; $NaHCO_3$, 0.1; NaCl, 28; ferric ammonium citrate, 0.006; citric acid, 0.006; Na_2 EDTA, 0.001 and 0.5 ml L^{-1} of trace metal solution. For biosorbent production, the strain was cultivated in 1-L bubbled flat glass bottles supplied by a sterile air/CO_2 mixture (99:1, v:v) at a flow rate of 0.2 L min^{-1} per L of culture with continuous illumination provided by a LED lamp with 200 μmol photons m^{-2} s^{-1}. The growth was monitored by optical density measurements at 680 nm (OD_{680}) and cell counting (cell mL^{-1}) adopting a Thoma counting chamber under an optical microscope. The harvested biomass was centrifuged (4000 rpm, 15 min) to obtain the cellular fraction (i.e., the pelletized cells resuspended in distilled water) and the soluble fraction (i.e., the EPS-rich supernatant) or used without centrifugation when the whole culture was needed. The different fractions or the whole culture were confined into dialysis tubing (MW cut-off 12–14 kDa, Medicell Membranes Ltd, UK) and pre-treated with an acidic solution (HCl 0.1M) as previously described by Ciani et al. (2024) to remove the excessive amount of salts contained in the cultivation medium. The same pre-treatment was carried out for dialysis tubing containing the cultivation medium (used as blank).

Cellular dry weight (i.e., the dry mass of the cellular fraction obtained after centrifugation and pre-treatment, DW, g L^{-1}) and carbohydrate concentration for each fraction (soluble carbohydrate, sCH_2O, and cellular carbohydrate, cCH_2O, g L^{-1}) were quantified as previously illustrated in Ciani et al. (2024). Briefly, cellular dry weight was quantified on pre-treated cellular fraction by filtration on dry pre-weighted MCE membrane filters (0.45 μm pore size, 47 mm diameter). The filters were then weighed after drying at 105 °C for 4 h. For carbohydrate quantification in the cellular and soluble fractions after pre-treatment, the phenol-sulfuric acid method (DuBois et al., 1956) was adopted.

2.2. Experimental set-up

To investigate the interaction between the metals and the cyanobacterium, a one-week grown culture (according to the preliminary assay described in the Supporting Information) was collected and treated for biosorbent preparation as described in the previous section. Pre-treated fractions were kept in contact with monometallic and multimetallic solutions as described in the following section (2.3), to investigate and compare the effect of different metals on metal binding properties related to biosorbent type (i.e. cellular or soluble fraction). After 24 h, metal-enriched biosorbents were mixed and freeze-dried before being chemically and structurally characterized. Finally, in order to find a new purpose for the generated metallic-organic materials, the catalytic properties of the metals sorbed on whole culture in the addition of bis(pinacolato)diboron to α,β-unsaturated chalcones were evaluated by optimizing reaction conditions.

2.3. Contact with metal ions solutions

Pre-treated fractions or the blank confined into dialysis tubing were dipped into aqueous solutions containing 10 mg L^{-1} of Cu(II), Ni(II), or/and Zn(II) obtained from stock solutions of 1 g L^{-1} Cu(II), Ni(II), Zn(II) using their respective chloride salts ($CuCl_2$, $NiCl_2$, and $ZnCl_2$). The three metals were added together when the multimetallic solution was tested. The biosorbent–sorbate ratio was 1:10 (v/v). A further test was conducted by dipping pre-treated fractions into distilled water (control). All the tests were continuously mixed for 24 h at a constant temperature (25 °C ± 1), maintained by controlling room temperature, and pH (5.0 ± 0.5), adjusted by adding NaOH or HCl 0.1M. In the following biosorption experiment, carried out to investigate the interaction of the metals with the soluble and cellular fractions, the biosorbents obtained after 24 h of contact with the metallic solutions were harvested and freeze-dried, metals were quantified on freeze-dried biomass by ICP-OES (inductively coupled plasma optical emission spectroscopy), and the samples were analyzed by SEM-EDX, FT-IR, and XAS. All analytical details are described in Supporting information.

2.4. General procedure for catalyzed addition of Bis(pinacolato)diboron on α,β-unsatured substrates

Freeze-dried metal-enriched materials adopted as catalysts (L-Me 10% mol equiv.) and $B_2(pin)_2$ (1.2 equiv.) were added to an anhydrous Schlenk under nitrogen atmosphere, then half of the required anhydrous MeOH was added (Fig. 1). The mixture was stirred for an hour at room temperature to activate the catalyst, and then the substrate and the remaining anhydrous MeOH were added. The stoichiometric catalyst: substrate:$B_2(pin)_2$ ratio was 1:10:12 or 1:5:6 to potentially enhance the catalytic activity of the cyanobacterial sample under examination.

The mixture was stirred at room temperature overnight under nitrogen atmosphere. It was then centrifuged at 6000 rpm for 8 min and the supernatant was evaporated under vacuum. Catalytic reactions were monitored by HPLC analysis with Jasco PU-2080 Plus equipped with UV detector Jasco UV-2075 Plus and AD-H Chiralcel and Lux cellulose column (Facchetti et al., 2020; Zanetti et al., 2022).

3. Results and discussion

The cellular and the soluble fractions of the cyanobacterium *D. salina* 16Som2, already known for its ability to remove metals (Ciani et al., 2024), were adopted to investigate the metal biosorption mechanisms and to characterize the chemical environment of the metals upon binding. The preliminary assay (results shown in Supporting Figure S1 and Figure S2), carried out to select the harvesting time of the biomass,

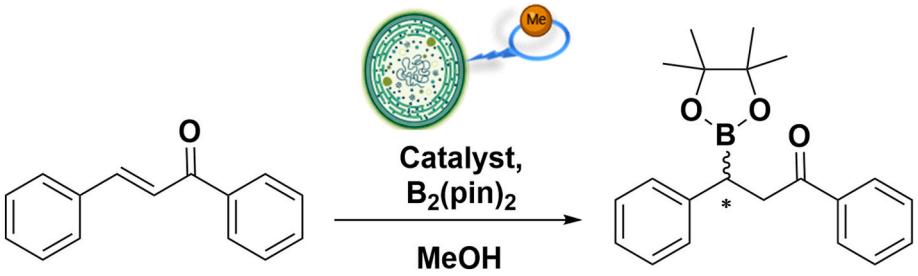

Fig. 1. General procedure for addition reaction of $B_2(pin)_2$ on chalcone.

revealed a decrease in specific metal uptake (expressed per gram of cellular dry weight or carbohydrate) using the biosorbents obtained from biomass cultivated for more than 7 days. Indeed, despite the highest Cu(II) removal efficiency (43%, Supporting Fig. S2) was attained by the soluble fraction at the end of the growth, the higher concentration of biosorbent can cause a reduction in specific metal uptake likely due to the saturation of available binding sites and the formation of aggregates in the biosorbent itself that reduces the surface area for metal interaction (De Philippis et al., 2011; Mota et al., 2016). Thus, the following biosorption experiment was carried out by adopting cellular and soluble fractions obtained from a 7-day grown culture.

3.1. Chemical and structural characterization of cyanobacteria-based biosorbents after contact with metal-containing solutions

3.1.1. Metal quantification, FT-IR spectroscopy and SEM-EDX analysis

The cellular and soluble fractions were collected and freeze-dried after being in contact with the Cu(II), Zn(II), Ni(II) and multimetallic solutions for their characterization. The elemental quantification performed via ICP-OES on the biomasses revealed that samples exposed to Cu(II) solution attained significantly higher metal concentrations compared to the others. Specifically, the elemental Cu content was 1.3–3.4 times higher than that of Ni or Zn (Table 1), reaching 7.02% (w/w) in the soluble fraction of the monometallic samples. Although Cu levels decreased in the multimetallic samples, the combined concentration of all three metals reached 8.76% (w/w), surpassing the concentrations achieved by any single metal in the monometallic samples.

It is worth mentioning that a reduction in the uptake of each metal when more than one is present in the solution is consistent with previous studies (Ciani et al., 2024; Pagnucco et al., 2023).

The metal biosorption potential of *D. salina* 16Som2 was previously investigated by Ciani et al. (2024) using whole culture. In that study, adsorption isotherms, which describe the equilibrium relationship between the metal bound to the biomass and its concentration in solution at a constant temperature, confirmed a high affinity for Cu(II). Notably, Cu(II) exhibited the highest *b* value, the Langmuir biosorption constant representing affinity and free adsorption energy, with a maximum adsorption capacity (q_{max}) of 33 mg Cu/g DW. The two controls were analyzed by FT-IR spectroscopy (Fig. S2), and SEM-EDX. SEM-EDX micrographs were compared to multimetallic samples (Fig. 2). The observation of the biosorbent based on the cellular fraction through SEM-EDX (Fig. 2a) revealed that the dominant peaks in the control were those of carbon (C) and oxygen (O), with minor amounts of phosphorus (P), sulfur (S), and calcium (Ca). The sample was compared with multimetallic sample (Fig. 2b), where Cu was visible instead of Ca, while Ni and Zn were not detected.

Table 1
Cu, Ni, and Zn content (%, w/w) in cellular and soluble fractions kept in contact with mono and multimetallic solutions.

Fraction	Test	Cu (%)		Ni (%)		Zn (%)	
		Average	St. Dev.	Average	St. Dev.	Average	St. Dev.
Cellular	Ctrl	0.03	0.01	0.00	0.00	0.05	0.00
	Multi	1.88	0.48	0.68	0.08	0.71	0.09
	Ni	0.05	0.01	1.97	0.03	0.04	0.01
	Cu	3.73	0.42	0.00	0.00	0.10	0.04
	Zn	0.05	0.02	0.00	0.00	1.10	0.07
Soluble	Ctrl	0.03	0.02	0.01	0.01	0.08	0.02
	Multi	4.25	0.94	2.28	0.14	2.23	0.11
	Ni	0.03	0.00	5.46	0.63	0.08	0.01
	Cu	7.02	0.87	0.00	0.00	0.07	0.01
	Zn	0.03	0.00	0.00	0.00	3.43	0.37

The structure of the soluble fraction appeared as layered, thin, and smooth sheets (Fig. 2c–d). The binding of metals can cause a reorganization of the EPS, as metal ions can bridge between functional groups in the polysaccharides (Flemming and Wingender, 2010), which appeared more fragmented and clumped after contact with metal ions. Similar to the cellular fraction, the dominant elements were C and O, with small amounts of sodium (Na), magnesium (Mg), P, S, and Ca. These elements are typical of the exopolysaccharide composition and the associated minerals from the cultivation medium (Ruffing, 2011). Cl content in metal-loaded samples increased, likely because all the tested metals were in the chlorinated form. In contrast to C and O, whose relative content remained roughly stable, the amount of the light metals decreased after contact with the multimetallic solution and Na disappeared from the spectra showing, instead, clear peaks for Cu, Ni, and Zn, suggesting that an ion-exchange mechanism may be involved in metal binding, as also demonstrated by Mota et al. (2016). The atomic and weight percentages of these elements followed the order Cu > Ni > Zn, in agreement with the ICP-OES quantification shown in Table 1. The higher affinity towards Cu(II) compared to Ni(II) and Zn(II) present in the solutions can be attributed to its flexible coordination chemistry (trigonal- and square-planar, tetrahedral and octahedral coordination), higher electronegativity, ability to form stronger and more stable complexes with functional groups like carboxyl, hydroxyl, and phosphate, which are abundant in cyanobacterial cell walls and EPS (Fomina and Gadd, 2014; Freire-Nordi et al., 2005; Gu and Lan, 2021; Hazarika et al., 2015; Salehizadeh and Shojaosadati, 2003). The ability of *D. salina* to retain Cu(II), Zn(II), and Ni(II) demonstrates its potential for addressing heavy metal contamination in water, highlighting a role in reducing the environmental impact of metal pollution.

3.1.2. XANES and EXAFS spectroscopy

XANES and EXAFS spectroscopy were adopted to explore the coordination environment of metals upon binding and to help identify the biological molecules and processes involved. The absorption edges in the XANES spectra of freeze-dried samples and model compounds were compared to determine the oxidation state of the metals after binding with cyanobacteria-based biosorbents. XANES results, shown for comparison in Fig. S4 (Supporting information), suggested that the oxidation state of Cu(II), Zn(II), and Ni(II) did not change upon binding, confirming their bivalent nature. The same behavior was observed also in previous studies investigating the interaction of metals with microbial biomasses and EPS adopting the same metals (Carr et al., 2017; Fang et al., 2011; Pokrovsky et al., 2012).

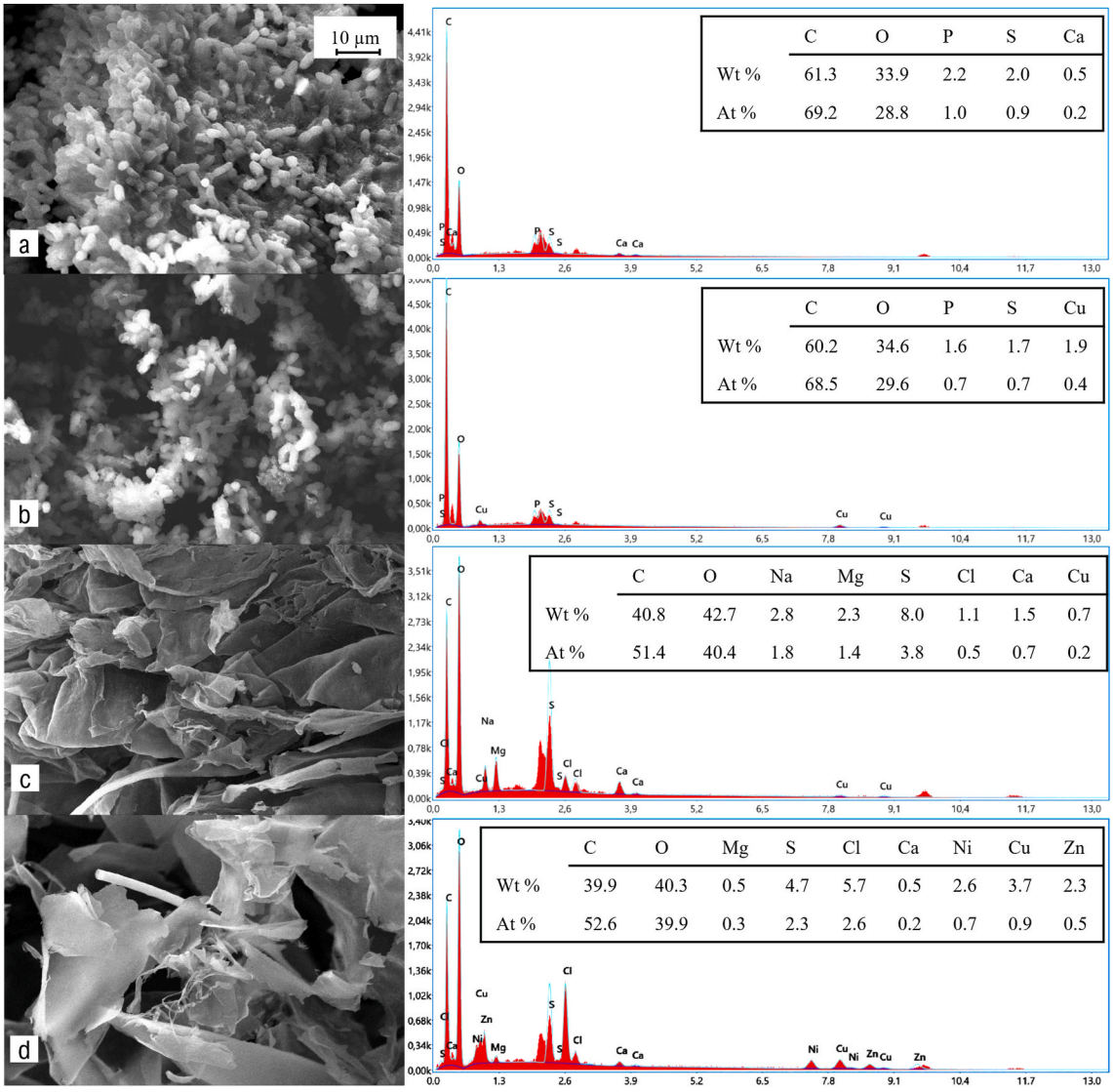

Fig. 2. SEM-EDX of cyanobacteria-based biosorbents, from the top: cellular fraction kept in contact with distilled water (a) and multimetallic solution (b); soluble fraction kept in contact with distilled water (c) and multimetallic solution (d). On the left, SEM micrographs (30000× magnification); on the right, the elementary microanalysis and the corresponding table summarizing the weight (Wt%) and atomic (At%) percentages of the detected elements.

EXAFS analysis was conducted to investigate the molecular environments of metals. It is worth mentioning that interpreting EXAFS spectra for metals within biological matrices is often challenging due to (i) distorted geometries and a variety of neighboring atoms (O, N, S, Cl) in the first coordination shell, (ii) the dominance of low atomic number elements (C, O, N) in the subsequent coordination shells, and (iii) static disorder which produces a high number of scattering pathways in metal–organic ligand structures yielding destructive interference and thus weak EXAFS signals (González et al., 2016). Furthermore, since the scattering power of elements is directly related to their atomic number, it is impossible to distinguish elements with similar Z such as C, N, O or S, Cl. Additionally, the coordination numbers derived from EXAFS have reduced accuracy due to their correlation with other parameters influencing the amplitude of the EXAFS oscillations, particularly the many-body amplitude reduction factor (S_0^2), which was fixed during fitting for this reason, and the Debye–Waller factor (σ^2). As a result, the data can be ambiguous, and an accuracy of approximately 20% is generally assumed for coordination numbers (Marmiroli et al., 2020).

Here, the coordination environment of the metals in all the studied samples was complex and affected by the presence of a combination of different atoms in the first shells, mainly (O,N) and (Cl,S). At first, the fittings were carried out by adopting only one type of ligand in the I coordination shell, letting the coordination number free to vary. Then, the fittings were repeated considering a mixed coordination and adopting the bond valence method (Brown and Altermatt, 1985) to investigate the ratio between different coordinating atoms according to their valence using the procedure reported in Marmiroli et al. (2020).

The main EXAFS parameters obtained with all combinations tested are shown in Table 2. The EXAFS and Fourier-transformed spectra of the measured samples are shown in Fig. S5 of supporting information.

The optimal fitting condition for each sample was selected based on the analysis of residuals in EXAFS and Fourier-transformed spectra, along with fitting statistics (reduced chi-squared and R-factor). When considering a mixed coordination led to a worsening in the fit, a simple single-binder model was employed. It is also worth remarking that the fitting approach here adopted accounts for three different scenarios: one in which the metal binds simultaneously to both light (O,N) and heavy elements (Cl,S) within the same coordination shell, another where it binds light or heavy elements in different coordination polyhedra, and a last one where the previous two scenarios coexist. Taking into account the accuracy of the fitted (O,N):(Cl,S) ratio we can distinguish five distinct (O,N):(Cl,S) configurations across the samples: only heavy

Table 2
EXAFS multiparameter fit details for the studied samples.

Fraction	Solution	k range (Å^{-1})	S_0^2	Path	R (Å)	N	v_i	O,N/Cl,S	σ^2 (Å^{-2})
Soluble	Cu(II)	2.9-12.5	0.80	Cu-O	1.93 (2)	3.94	0.51	0.46 (17)	0.003 (2)
				Cu-Cl	2.20 (2)	3.39	0.59		0.012 (2)
				Cu-O	1.92 (2)	3.83	0.52	0.30 (20)	0.015 (2)
				Cu-S	2.18 (3)	4.80	0.42		0.001 (3)
				Cu-N	1.93 (2)	4.74	0.42	0.21 (15)	0.000 (3)
				Cu-S	2.17 (2)	4.67	0.43		0.014 (1)
				Cu-N	1.94 (2)	4.88	0.41	0.37 (14)	0.002 (2)
				Cu-Cl	2.19 (2)	3.31	0.60		0.011 (2)
Soluble	Cu(II) (multi)	2.9-12.5	0.80	Cu-O	1.93 (2)	3.92	0.51	0.44 (19)	0.002 (2)
				Cu-Cl	2.20 (2)	3.46	0.58		0.010 (2)
				Cu-O	1.91 (2)	3.74	0.53	0.23 (18)	0.000 (3)
				Cu-S	2.19 (3)	4.83	0.41		0.013 (1)
				Cu-N	1.92 (2)	4.69	0.43	0.21 (17)	0.000 (3)
				Cu-S	2.18 (2)	4.75	0.42		0.013 (1)
				Cu-N	1.94 (2)	4.84	0.41	0.36 (15)	0.001 (2)
				Cu-Cl	2.19 (2)	3.36	0.59		0.009 (1)
Cellular	Cu(II)	2.9-12.5	0.80	Cu-O	1.94 (2)	4.02	0.50	0.72 (23)	0.004 (2)
				Cu-Cl	2.20 (5)	3.44	0.58		0.013 (6)
				Cu-O	1.93 (2)	4.00	0.50	0.69 (26)	0.004 (2)
				Cu-S	2.20 (5)	5.06	0.39		0.016 (6)
				Cu-N	1.94 (2)	4.94	0.41	0.57 (25)	0.003 (2)
				Cu-S	2.19 (4)	4.89	0.41		0.015 (4)
				Cu-N	1.95 (2)	4.97	0.40	0.63 (22)	0.003 (2)
				Cu-Cl	2.19 (4)	3.35	0.60		0.011 (4)
Cellular	Cu(II) (multi)	2.9-12.5	0.80	Cu-O	1.95 (2)	4.21	0.47	0.66 (24)	0.004 (2)
				Cu-Cl	2.19 (5)	3.37	0.59		0.016 (9)
				Cu-O	1.95 (2)	4.19	0.48	0.64 (27)	0.004 (2)
				Cu-S	2.20 (5)	4.98	0.40		0.019 (9)
				Cu-N	1.94 (2)	4.91	0.41	0.55 (28)	0.015 (25)
				Cu-S	2.18 (5)	4.74	0.42		0.010 (2)
				Cu-N	1.96 (2)	5.18	0.39	0.55 (23)	0.003 (2)
				Cu-Cl	2.19 (5)	3.21	0.60		0.014 (6)
Soluble	Zn(II)	2.9-11.4	0.90	Zn-O	1.93 (10)	3.75	0.53	0.48 (43)	0.004 (9)
				Zn-Cl	2.21 (4)	3.45	0.58		0.005 (6)
				Zn-O	1.97 (3)	4.22	0.47	0.57 (19)	0.005 (2)
				Zn-S	2.25 (2)	3.10	0.65		0.003 (2)
				Zn-N	1.99 (9)	3.61	0.55	0.61 (67)	0.001 (5)
				Zn-S	2.25 (6)	3.04	0.66		0.000 (8)
				Zn-N	1.96 (11)	3.32	0.60	0.50 (42)	0.000 (7)
				Zn-Cl	2.21 (7)	3.44	0.58		0.003 (9)
Soluble	Zn(II) (multi)	3.2-13.0	0.90	Zn-Cl	2.24 (0)	3.73	0.54	0	0.005 (3)
				Zn-S	2.26 (1)	4.16	0.62	0	0.005 (1)
Cellular	Zn(II)	3.0-12.5	0.90	Zn-O	1.96 (5)	4.08	0.49	0.58 (34)	0.005 (4)
				Zn-Cl	2.24 (3)	3.75	0.53		0.004 (3)
				Zn-O	1.98 (3)	4.36	0.46	0.64 (22)	0.006 (3)
				Zn-S	2.27 (2)	3.28	0.61		0.003 (3)
				Zn-N	2.01 (8)	3.80	0.53	0.64 (64)	0.002 (5)
				Zn-S	2.26 (5)	3.18	0.63		0.001 (7)
				Zn-N	1.97 (10)	3.56	0.56	0.49 (82)	0.001 (7)
				Zn-Cl	2.23 (6)	3.59	0.56		0.004 (9)
Cellular	Zn(II) (multi)	3.2-12.8	0.90	Zn-Cl	2.27 (1)	4.13	0.49	0	0.006 (8)
				Zn-S	2.28 (4)	4.59	0.63	0	0.006 (5)
Soluble	Ni(II)	2.7-12.0	0.95	Ni-O	2.05 (1)	5.64	0.35	1	0.005 (1)
			1.00	Ni-N	2.07 (1)	6.20	0.32	1	0.005 (1)
Soluble	Ni(II) (multi)	2.4-11.7	0.98	Ni-O	2.05 (1)	5.72	0.35	1	0.006 (1)
			0.99	Ni-N	2.07 (1)	6.31	0.32	1	0.006 (1)
Cellular	Ni(II)	2.5-11.8	0.95	Ni-O	2.06 (1)	5.77	0.35	1	0.006 (1)
			0.97	Ni-N	2.08 (1)	6.36	0.31	1	0.006 (1)
Cellular	Ni(II) (multi)	2.5-11.8	1.00	Ni-O	2.06 (1)	5.83	0.34	1	0.007 (1)
			1.01	Ni-N	2.08 (1)	6.42	0.31	1	0.007 (1)

Notes: S_0^2 = many-body amplitude reduction factor (fixed on the base of the fitting carried out on reference compounds, except for Ni(II)-samples). N = path degeneracy. v_i = valence. R = path length. σ^2 = Debye–Waller factor. Uncertainties of the fit are shown within parentheses. 0 and 1 in the **O,N/Cl,S** column indicate that (O,N) or (Cl,S) bonds, respectively, were not detected.

elements (Cl,S) or only light elements (O,N) in the first coordination shell, with a value of 0 or 1, respectively; a predominance of heavy elements within the same or different coordination polyhedron (ratio ~ 0.25); an even distribution of heavy and light elements (ratio ~ 0.5); and mostly light elements (ratio ~ 0.75).

The fit results revealed that the Cu(II)–(O,N) and Cu(II)–(Cl,S) average bond distances were consistent across all samples, with ranges of 1.91–1.96 Å and 2.17–2.20 Å, respectively. The coordination numbers (*N*) varied between 3.83 and 5.12 for (O,N), and between 3.21 and 5.06 for (Cl,S) with higher coordination numbers with N or S. These results agree with those observed by different authors that found Cu(II) in a square planar coordination with oxygen after sorption with cyanobacterial or microalgal biomass (Belle et al., 2005; Pokrovsky et al., 2012). Nevertheless, the Cu(II) geometry in coordination with (O,N) is often regarded as pseudo-octahedral, with four equatorial strongly bounded atoms and two axial ligands with longer and looser bonds due to the Jahn-Teller effect (Pokrovsky et al., 2012). Despite some attempts to include axial O atoms in the fits, their contribution was very weak without a significant improvement.

The (O,N):(Cl,S) ratio in the cellular fraction was higher than in the soluble fraction, suggesting the presence of more Cu(II)-(O,N) interactions than Cu(II)-(Cl,S). A slight decrease in the (O,N):(Cl,S) ratio was observed in multimetallic systems compared to monometallic systems. The attempts to fit next-nearest coordination shell features resulted in difficult interpretation due to a weak signal as well as complex distribution of different elements. The addition of Cu–Cu scattering paths at higher distances (3.40–3.90 Å, *N* 4-6) improved the fits of all EXAFS spectra. Knowing that in biological systems 35 % of Cu ligands are cysteine residues (Wu et al., 2010), it is possible to suppose the presence of S ligand more than Cl ligand in the cellular fraction. Nevertheless, it's not possible to distinguish intracellular and extracellular ligands that may influence the (O,N):(Cl,S) ratio.

For Zn(II), the most evident difference among samples is the absence of (O,N) atoms in the nearest neighbors after exposure to the multimetallic solution ((O,N):(Cl,S) ratio 0) with an increase in Zn(II)-(Cl,S) distances and coordination number (2.24-2.28 Å, *N* 3.73-4.19). Indeed, the addition of Zn(II)-(O,N) paths in the fitting of multimetallic samples did not contribute to the fitting. This huge decrease in the (O,N):(Cl,S) ratio compared to the value of the monometallic samples (~0.5 or slightly higher depending on the combinations) may suggest a higher affinity of (O,N) atoms towards the other metals and of (Cl,S) toward Zn (II). In samples treated with Zn(II)-only solutions, Zn(II)–(O,N) bond distances ranged from 1.93 to 2.01 Å, with coordination numbers between 3.32 and 4.36, while Zn(II)–(Cl,S) bond distances ranged from 2.21 to 2.28 Å, with coordination numbers between 3.45 and 4.09. The soluble fraction containing released polysaccharides is characterized by higher structural flexibility compared to the more tightly packed, structured environment typical of cells, where metals might interact with specific, well-defined sites leading to weaker or more distant metal-ligand interactions, resulting in longer bond distances. This may explain the higher distances exhibited in the soluble fraction. Zn has already been found in tetrahedral coordination as Zn phosphate or oxalate in several biological materials (Pokrovsky et al., 2005) but it is also known that it can easily bind to sulfur (Vanzile et al., 2000). In this study, second next-nearest shell features may correspond to O/C/N atoms (3.80–3.99 Å, *N* 4-8), thus suggesting that Zn(II) may bind to carboxylate or sulfur-containing groups.

In contrast to Cu(II) and Zn(II), the EXAFS fitting for Ni(II) revealed the absence of Cl or S atoms in the first coordination sphere of all samples ((O,N):(Cl,S) ratio 1). Instead, Ni(II) was coordinated with 5.64–6.42 (O,N) atoms at 2.05-2.08 Å, suggesting an octahedral geometry, unlike the square planar or tetrahedral geometries observed for Cu (II) and Zn(II), characterized by lower coordination numbers. The lower Ni(II) absorption compared to Cu(II) (Table 1) along with the observed decrease in the O/Cl ratio in Cu(II)-samples after exposure to multimetallic systems, may be attributed to the higher oxygen demand for Ni (II) coordination. In this case, the addition of Ni(II)-Ni (2.91-2.95 Å, *N* 2) and Ni(II)-S (4.09-4.28 Å, *N* 6) scattering paths after first coordination shells, improved the fits of all EXAFS spectra, suggesting the presence of S containing groups (e.g., sulfate groups). Information on Ni interaction with biological materials is scarce. It is known that cyanobacteria possess some metalloregulators that are Ni-responsive members, but a planar four-coordinate structure has been found for these molecules (Carr et al., 2017), contrarily to the result obtained in this study. However, Montargès-Pelletier et al. (2008) observed that carboxylic acids appeared as the main Ni ligands in plants resulting in a coordination 6 with O atoms at 2.03-2.06 Å. Those results are consistent with what was observed in the current study, suggesting the involvement of carboxylic acids in Ni(II) ligation.

Cu(II), Ni(II), and Zn(II) distances here reported exclude the involvement of van der Waals forces in favour of covalent or ionic bonds. Indeed, van der Waals interactions, which are weak and non-bonding, typically manifest at longer interatomic distances (Alvarez, 2013). Various authors have tentatively attributed the EXAFS features of next-nearest coordination shells in biological materials to C, P, or S atoms at distances of 2.0–3.2 Å (Fang et al., 2011; Pokrovsky et al., 2012). The distances reported by the authors are shorter than those observed in the current study. Nevertheless, it is worth mentioning that a weak signal—potentially caused by destructive interference—may hide certain features. Although all path combinations were tested, the results suggest that O and Cl coordination paths were most likely in soluble fraction as also supported by the observed increase in Cl content following exposure to the multimetallic solution shown by EDX microanalysis (Fig. 2). Similarly, Adams et al. (2021) proposed a complexation mechanism with a mixed coordination sphere containing N and Cl atoms for Au(III) supplied as $AuCl_3$ onto the surface of the alga *Galdieria sulphuraria* cells by EXAFS analysis. Despite adopting O and Cl paths resulted in good fit parameters also in the cellular fraction, O and S paths also exhibited good fit results. Additionally, contrarily to the soluble fraction, no clear Cl peak was observed in EDX microanalysis and S is known to participate in metal binding in biological systems. Indeed, copper and zinc sulfur ligation is involved in different metalloenzymes and proteins (Belle et al., 2005; Cassier-Chauvat and Chauvat, 2015). It should be noted, however, that these fittings do not rule out the potential presence of both atoms (Cl and S, O and N), suggesting an even more complex coordination environment, which aligns with the inherent complexity of biological materials. Furthermore, it must be highlighted that metal speciation is influenced by the pH of the working conditions but also by the extracellular adsorption or intracellular assimilation (González et al., 2016). The distinct observed metal-binding preferences highlight the adaptability of the biosorbent to various metal types, enabling versatile applications in pollutant remediation. To investigate metal binding properties with more detail, more studies are needed to investigate metal localization and interactions in the cells at a smaller scale.

3.2. Catalytic activity

3.2.1. Catalytic potential and reaction's optimization

In order to find a new purpose for metal-enriched cyanobacteria, promoting waste valorization, freeze-dried samples were tested for their catalytic activity in a reaction of pharmaceutical interest. Preliminary data acquired on both the cellular and soluble fractions after contact with Cu(II) did not show any relevant difference in terms of reactivity.

Thus, the following experiments were carried out using whole cultures exposed to metal-containing solutions.

A comparison of the data acquired during the tests indicates that the different samples of cyanobacteria display unmistakably dissimilar behaviors when exposed to the same reactants (chalcone and $B_2(pin)_2$) under identical experimental conditions (Fig. 3).

The initial tests conducted with *D. salina* 16Som2 without exposure to metals (ctrl) provided a conversion rate of around 30% (mean value) measured via HPLC (Fig. 3), implying that the addition of boron to an α,β-unsaturated chalcone is a chemical transformation that spontaneously happens to an extent, even in the absence of a real catalyst, and likely due to the addition of MeOH to the reaction environment. Indeed, this polar and protic solvent acts as a proton donor, promoting the reaction. The values obtained in these initial tests were used as a benchmark to evaluate the catalytic activity of all the samples containing metals. The use of different metal cations bound to the cyanobacterium exhibited contrasting effects on the conversion rates of the β-borylation of chalcone (Fig. 3). The most interesting behavior was observed in the Cu(II)-sample leading to 94% (mean value of triplicate experiments) conversion rate, measured by HPLC.

This result is characterized by a high standard deviation due to the inevitable heterogeneity of the samples. On the other hand, Ni(II)-enriched samples did not exhibit any conversion of the substrate while Zn(II)-enriched samples showed an intermediate behavior: at low concentrations, the reactivity resulted very low while decreasing the substrate:metal catalyst ratio, the situation reversed, demonstrating a clear catalytic effect.

The data collected from tests containing multi-metal samples were also interesting, as they exhibited slightly inferior catalytic activity compared to Cu(II)-enriched samples.

The different behavior of metal-enriched samples obtained after biosorption of different metals may be related to the different chemical and structural environment as explained in the previous section. Indeed, it is known that multiple factors related to the coordination environment, including metal size and ligands, influence the catalytic reactions (Bullock and Dey, 2022; Zhang et al., 2020). Here, the catalytic performances according to the metals follow the order Cu > Cu + Zn + Ni > Zn > Ni. This order is consistent with the structure of 1st coordination shell of the samples. Indeed, if Cu(II) and Zn(II) were coordinated with ~4 (O,N) and (Cl,S) atoms at different ratios depending on the fraction, Ni(II) was coordinated with ~6 (O,N) atoms. Therefore, the absence of catalytic activity of Ni(II)-enriched samples may be due to the preference shown by Ni(II) to bond only oxygen atoms in octahedral geometry. This in turn leads to fewer available sites and restricted flexibility in the interaction with substrates. Also, in situ stabilization of the Ni(0) catalyst and competition between boronic acid formation and transmetalation with the oxidative addition complex could further contribute to the observed loss of reactivity (Molander et al., 2013). Nevertheless, to confirm this hypothesis, further studies are needed to investigate the role of the coordination environment, including next-nearest coordination shells, and the accessibility of metals bound to cyanobacteria-based biosorbents in catalysis.

To optimize the reaction, a screening was realized to identify the ideal reaction conditions that would nullify the conversion observed in

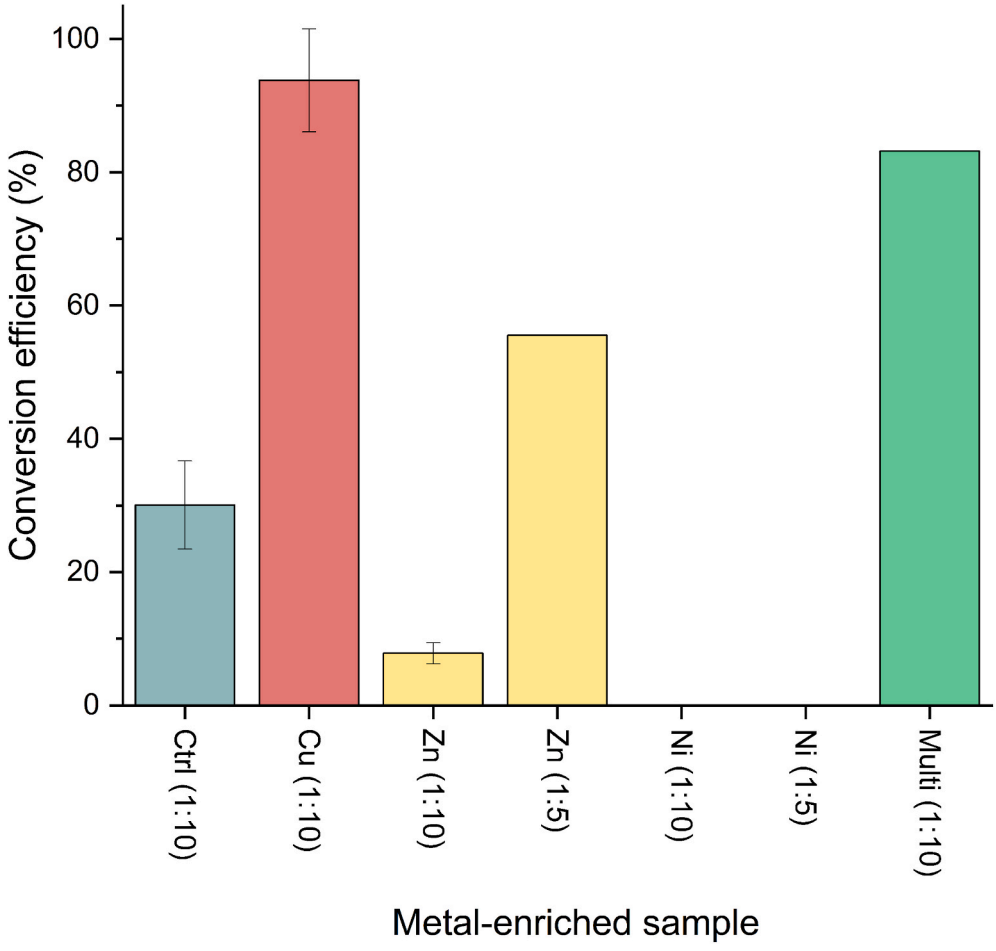

Fig. 3. Conversion efficiency of 16Som2-metal catalysts obtained after contact with different metals in the addition reaction of $B_2(pin)_2$ on chalcone. The conversion was evaluated by HPLC using analytical conditions reported in literature (Gandolfi et al., 2022). In brackets, the catalyst:substrate ratio is reported. HPLC chromatograms for all the substrates with analysis conditions employed and retention time of starting material and products are shown in Supporting Information.

tests with control samples to exclusively appreciate the catalytic activity exhibited by Cu(II). Therefore, diethyl ether was introduced as cosolvent to reduce the amount of methanol required by the reaction to work as an activator without catalyzing any transformation when metals are not present in the samples. The optimal methanol:diethyl ether ratio was set at 1.5:1. Under these conditions, the Cu(II)-enriched samples yielded an average conversion of 87%.

Using the optimized reaction conditions, the data collected with multimetallic samples showed again slightly inferior catalytic activity compared to that of Cu(II)-enriched samples. The conversion rate calculated via HPLC analysis was 82%, which was higher than the value obtained in the tests conducted with the control cells (12% yield) and comparable to that using Cu(II)-enriched samples (87% yield) under the same experimental conditions. This confirmed a potential synergistic activity of the metals, capable of partially balancing the reduced percentage of copper, which still requires further investigation. The catalytic performance of Cu(II)- and multimetal-enriched samples not only underscores the feasibility of repurposing biosorbents but also offers an environmentally friendly alternative to traditional catalysts in green chemistry.

3.2.2. *Catalytic activity of multimetallic sample on differently functionalized chalcones*

After confirming that the most promising hybrid catalysts were those containing either copper or all three metals (Cu(II), Ni(II) and Zn(II)), it was decided to use the latter to catalyze the same borylation reaction on differently functionalized chalcones, to evaluate if the presence of a substituent on one of the two benzene rings, in the *meta* or *para* position, could modify the reactivity of the molecule (Fig. 4). Indeed, considering the future applicability of this approach, the multimetallic samples would mimic more closely the final product of the biosorption process, carried out on real, complex effluents where more than one metal is usually present, whose application as new valuable catalysts would fulfill the circular economy principles.

As depicted in Fig. 4, the addition of functional groups such as chlorine (*meta* and *para* substituted) and nitro (*meta* substituted) had no impact on the catalytic activity: as a matter of fact, the mean values of the conversion rates obtained were above 90%, confirming that the functionalization of chalcone, regardless of the nature and the position of substituents, had no influence on the capability of multimetallic samples to catalyze the β-borylation of the substrate and that these new catalytic methods are valid and robust.

4. Conclusions

This study demonstrates the potential of cyanobacteria-based biosorbents, derived from *Dactylococcopsis salina*, as a sustainable strategy for both heavy metal removal and waste valorization. Biosorption capability by *D. salina* 16Som2 was higher for Cu(II), reaching 3.7% and 7.0% (w/w) in the cellular and soluble (EPS-rich) fractions, respectively. Advanced structural analysis through EXAFS and XANES elucidated distinct coordination environments for each metal: *i)* Cu(II) exhibited four-fold coordination with (O,N):(Cl,S) ratio of 0.5 in the soluble fraction and 0.75 in the cellular fraction; *ii)* Zn(II) also showed four-fold coordination, but its (O,N):(Cl,S) ratio of 0.5 dropped to 0 in multimetallic systems, indicating a shift toward heavy-ligand (Cl, S) binding; *iii)* Ni(II) was found to be six-fold coordinated, bonded exclusively to O/N ligands regardless of the fraction or the presence of other metals.

Finally, the study successfully demonstrated the catalytic valorization of this metal-enriched biomass. In the borylation of α,β-unsaturated chalcones, Cu(II)- and multimetal-enriched biosorbents achieved outstanding catalytic activity with conversion efficiencies up to 94%. These results establish that the specific chemical coordination of the biosorbed metal directly dictates its subsequent catalytic performance.

By integrating bioremediation with catalyst development, this study contributes to sustainable, cleaner production, addressing environmental pollution while recycling biosorbed metals through generation of value-added materials for pharmaceutical applications. Further research should focus on the scale-up of the process, expanding this strategy to other metals and reactions to enhance its environmental and industrial impact while evaluating its environmental safety.

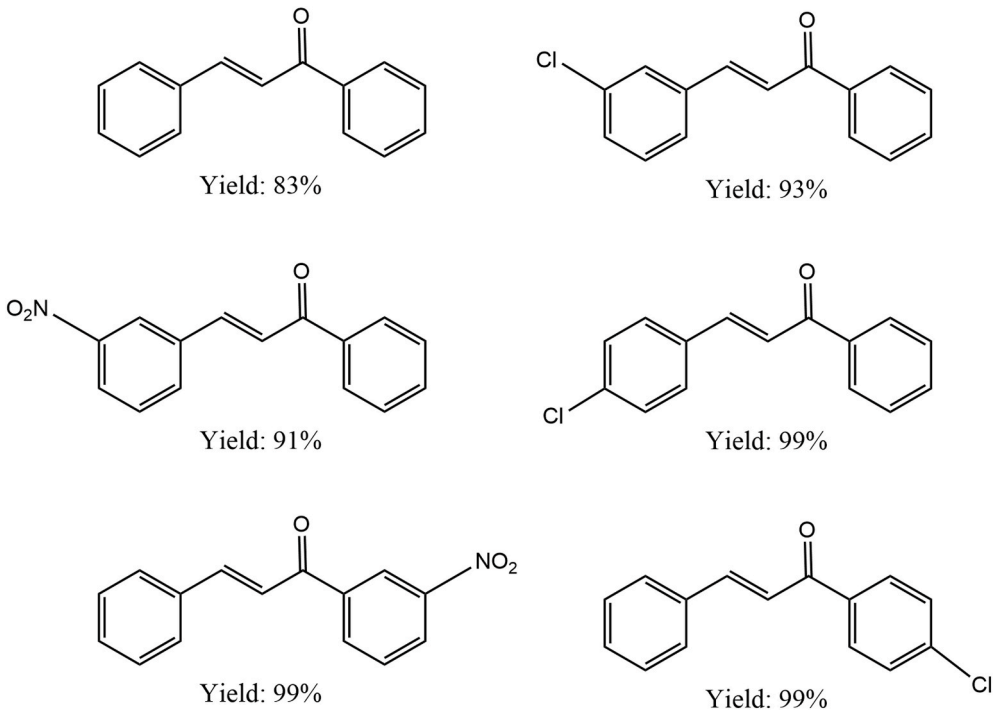

Fig. 4. Addition reaction of $B_2(pin)_2$ on six differently substituted α,β-unsaturated chalcones adopting multimetallic-sample. The yield for each reaction is indicated as conversion efficiency (%).

CRediT authorship contribution statement

Matilde Ciani: Writing – original draft, Methodology, Investigation, Data curation, Conceptualization. **Giovanni Orazio Lepore:** Writing – review & editing, Supervision, Methodology, Investigation, Funding acquisition, Data curation, Conceptualization. **Giorgio Facchetti:** Writing – review & editing, Supervision, Methodology, Investigation, Data curation, Conceptualization. **Karima Guehaz:** Writing – review & editing, Investigation. **Alessandro Puri:** Writing – review & editing, Investigation. **Raffaella Gandolfi:** Writing – review & editing, Supervision, Methodology, Investigation, Data curation, Conceptualization. **Isabella Rimoldi:** Writing – review & editing, Supervision, Methodology, Investigation, Data curation, Conceptualization. **Roberto De Philippis:** Writing – review & editing, Supervision. **Alessandra Adessi:** Writing – review & editing, Supervision, Methodology, Funding acquisition, Conceptualization.

Funding sources

This work was supported by Fondazione CARIPLO-Circular Economy 2020 Project num. 1069- 2020 "Heavy Metal Bio-recovery and Valorization-HMBV" (https://sites.unimi.it/hmbv/), by the COMBINE project funded by the University of Florence in the frame of "Competitive call of biannual projects for Temporary Researchers, edition 2024- 2025 (D.R. n. 419 May 02, 2023)", and "One Health Action Hub: University Task Force for the resilience of territorial ecosystems" funded by Università degli Studi di Milano–PSR 2021-GSA-Linea 6.

Declaration of competing interest

The authors declare the following financial interests/personal relationships which may be considered as potential competing interests: Alessandra Adessi reports financial support was provided by Fondazione CARIPLO. If there are other authors, they declare that they have no known competing financial interests or personal relationships that could have appeared to influence the work reported in this paper.

Acknowledgments

The authors acknowledge Dott. Simone Margheri from University of Florence for his contribution to the work; the Federation of European Microbiological Societies (FEMS) for the financial support received by FEMS Research and Training Grant; ESRF, Dott. Francesco d'Acapito and the Italian CRG beamline at ESRF (LISA-BM08) for the provision of beam-time and assistance during the experiment (Experiment #EV-514, Ciani, M., Lepore, G. O., Margheri, S. (2026). Chemical and structural characterization of metal-organic materials obtained through heavy metal biosorption by exopolysaccharide-producing cyanobacteria. European Synchrotron Radiation Facility. https://doi.org/10.15151/ESRF-ES-1234126108).

Appendix A. Supplementary data

Supplementary data to this article can be found online at https://doi.org/10.1016/j.jclepro.2026.147741.

Data availability

Data will be made available on request.

References

Adams, E., Maeda, K., Kato, T., Tokoro, C., 2021. Mechanism of gold and palladium adsorption on thermoacidophilic red alga *Galdieria sulphuraria*. Algal Res. 60, 102u49. https://doi.org/10.1016/j.algal.2021.102549.

Al-Amin, A., Parvin, F., Chakraborty, J., Kim, Y.-I., 2021. Cyanobacteria mediated heavy metal removal: a review on mechanism, biosynthesis, and removal capability. Environ. Technol. Rev. 10, 44–57. https://doi.org/10.1080/21622515.2020.1869323.

Alvarez, S., 2013. A cartography of the van der Waals territories. Dalton Trans. 42, 8617–8636. https://doi.org/10.1039/C3DT50599E.

Bădescu, I.S., Bulgariu, D., Ahmad, I., Bulgariu, L., 2018. Valorisation possibilities of exhausted biosorbents loaded with metal ions – a review. J. Environ. Manag. 224, 288–297. https://doi.org/10.1016/j.jenvman.2018.07.066.

Belle, C., Rammal, W., Pierre, J.-L., 2005. Sulfur ligation in copper enzymes and models. J. Inorg. Biochem. 99, 1929–1936. https://doi.org/10.1016/j.jinorgbio.2005.06.013.

Brown, I.D., Altermatt, D., 1985. Bond-valence parameters obtained from a systematic analysis of the inorganic crystal structure database. Acta Crystallogr. B 41, 244–247. https://doi.org/10.1107/S0108768185002063.

Bullock, R.M., Dey, A., 2022. Introduction: catalysis beyond the first coordination sphere. Chem. Rev. 122, 11897–11899. https://doi.org/10.1021/acs.chemrev.2c00428.

Carr, C.E., Foster, A.W., Maroney, M.J., 2017. An XAS investigation of the nickel site structure in the transcriptional regulator InrS. J. Inorg. Biochem. 177, 352–358. https://doi.org/10.1016/j.jinorgbio.2017.08.003.

Cassier-Chauvat, C., Chauvat, F., 2015. Responses to oxidative and heavy metal stresses in cyanobacteria: recent advances. Int. J. Mol. Sci. 16, 871–886. https://doi.org/10.3390/ijms16010871.

Chai, Y., Chen, A., Bai, M., Peng, L., Shao, J., Yuan, J., Shang, C., Zhang, J., Huang, H., Peng, C., 2022. Valorization of heavy metal contaminated biomass: recycling and expanding to functional materials. J. Clean. Prod. 366, 132771. https://doi.org/10.1016/j.jclepro.2022.132771.

Chakdar, H., Thapa, S., Srivastava, A., Shukla, P., 2022. Genomic and proteomic insights into the heavy metal bioremediation by Cyanobacteria. J. Hazard Mater. 424, 127609. https://doi.org/10.1016/j.jhazmat.2021.127609.

Chauhan, D., Prasad, P., Sasmal, P.K., 2024. Organoiridium-catalyzed bioorthogonal chemistry. Coord. Chem. Rev. 520, 216139. https://doi.org/10.1016/j.ccr.2024.216139.

Ciani, M., Adessi, A., 2023. Cyanoremediation and phyconanotechnology: cyanobacteria for metal biosorption toward a circular economy. Front. Microbiol. 14.

Ciani, M., Decorosi, F., Ratti, C., De Philippis, R., Adessi, A., 2024. Semi-continuous cultivation of EPS-producing marine cyanobacteria: a green biotechnology to remove dissolved metals obtaining metal-organic materials. N. Biotech. 82, 33–42. https://doi.org/10.1016/j.nbt.2024.04.004.

Compagno, N., Profeta, R., Scarso, A., 2023. Recent advances in the synthesis of active pharmaceutical and agrochemical ingredients in micellar media. Curr. Opin. Green Sustainable Chem. 39, 100729. https://doi.org/10.1016/j.cogsc.2022.100729.

De Philippis, R., Colica, G., Micheletti, E., 2011. Exopolysaccharide-producing Cyanobacteria in heavy metal removal from water: molecular basis and practical applicability of the biosorption process. Appl. Microbiol. Biotechnol. 92, 697–708. https://doi.org/10.1007/s00253-011-3601-z.

Diankristanti, P.A., Ng, I.-S., 2024. Marine microalgae for bioremediation and waste-to-worth valorization: recent progress and future prospects. Blue Biotechnol. 1, 10. https://doi.org/10.1186/s44315-024-00010-w.

Do Nascimento, M., Battaglia, M.E., Sanchez Rizza, L., Ambrosio, R., Arruebarrena Di Palma, A., Curatti, L., 2019. Prospects of using biomass of N2-fixing Cyanobacteria as an organic fertilizer and soil conditioner. Algal Res. 43, 101652. https://doi.org/10.1016/j.algal.2019.101652.

DuBois, Michel, Gilles, K.A., Hamilton, J.K., Rebers, P.A., Smith, Fred, 1956. Colorimetric method for determination of sugars and related substances. Anal. Chem. 28, 350–356. https://doi.org/10.1021/ac60111a017.

Facchetti, G., Christodoulou, M.S., Binda, E., Fusè, M., Rimoldi, I., 2020. Asymmetric hydrogenation of 1-aryl substituted-3,4-Dihydroisoquinolines with iridium catalysts bearing different phosphorus-based ligands. Catalysts 10, 914. https://doi.org/10.3390/catal10080914.

Facchetti, G., Rimoldi, I., 2018. 8-Amino-5,6,7,8-tetrahydroquinoline in iridium(iii) biotinylated Cp* complex as artificial imine reductase. New J. Chem. 42, 18773–18776. https://doi.org/10.1039/C8NJ04558E.

Facchetti, G., Vitoria, J.G., Moraschi, M., Bucci, R., Abel, A.C., Pieraccini, S., Pellegrino, S., Rimoldi, I., 2023. Exploitation of dimeric cyclic cysteine as helix inducer in ultra-short peptides for Cu(II)-Catalyzed asymmetric michael addition on chalcones. Eur. J. Org Chem. 26, e202300240. https://doi.org/10.1002/ejoc.202300240.

Fang, L., Zhou, C., Cai, P., Chen, W., Rong, X., Dai, K., Liang, W., Gu, J.-D., Huang, Q., 2011. Binding characteristics of copper and cadmium by cyanobacterium Spirulina platensis. J. Hazard Mater. 190, 810–815. https://doi.org/10.1016/j.jhazmat.2011.03.122.

Flemming, H.-C., Wingender, J., 2010. The biofilm matrix. Nat. Rev. Microbiol. 8, 623–633. https://doi.org/10.1038/nrmicro2415.

Fomina, M., Gadd, G.M., 2014. Biosorption: current perspectives on concept, definition and application. Bioresour. Technol. 160, 3–14. https://doi.org/10.1016/j.biortech.2013.12.102.

Franco-Morgado, M., Amador-Espejo, G.G., Pérez-Cortés, M., Gutiérrez-Uribe, J.A., 2023. Microalgae and Cyanobacteria polysaccharides: important link for nutrient recycling and revalorization of agro-industrial wastewater. Appl. Food Res. 3, 100296. https://doi.org/10.1016/j.afres.2023.100296.

Freire-Nordi, C.S., Vieira, A.A.H., Nascimento, O.R., 2005. The metal binding capacity of *Anabaena spiroides* extracellular polysaccharide: an EPR study. Process Biochem. 40, 2215–2224. https://doi.org/10.1016/j.procbio.2004.09.003.

Gandolfi, R., Facchetti, G., Cavalca, L., Mazzini, S., Colombo, M., Coffetti, G., Borgonovo, G., Scaglioni, L., Zecchin, S., Rimoldi, I., 2022. Hybrid catalysts from copper biosorbing bacterial strains and their recycling for catalytic application in the

asymmetric addition reaction of B2(pin)2 on α,β-Unsaturated chalcones. Catalysts 12, 433. https://doi.org/10.3390/catal12040433.
González, A.G., Jimenez-Villacorta, F., Beike, A.K., Reski, R., Adamo, P., Pokrovsky, O.S., 2016. Chemical and structural characterization of copper adsorbed on mosses (Bryophyta). J. Hazard Mater. 308, 343–354. https://doi.org/10.1016/j.jhazmat.2016.01.060.
Gu, S., Lan, C.Q., 2021. Biosorption of heavy metal ions by green alga neochloris oleoabundans: effects of metal ion properties and cell wall structure. J. Hazard Mater. 418, 126336. https://doi.org/10.1016/j.jhazmat.2021.126336.
Hafeez, J., Bilal, M., Rasool, N., Hafeez, U., Adnan Ali Shah, S., Imran, S., Amiruddin Zakaria, Z., 2022. Synthesis of ruthenium complexes and their catalytic applications: a review. Arab. J. Chem. 15, 104165. https://doi.org/10.1016/j.arabjc.2022.104165.
Hazarika, J., Pakshirajan, K., Sinharoy, A., Syiem, M.B., 2015. Bioremoval of Cu(II), Zn (II), Pb(II) and Cd(II) by Nostoc muscorum isolated from a coal mining site. J. Appl. Phycol. 27, 1525–1534. https://doi.org/10.1007/s10811-014-0475-3.
Iacovino, L.G., Pinzi, L., Facchetti, G., Bortolini, B., Christodoulou, M.S., Binda, C., Rastelli, G., Rimoldi, I., Passarella, D., Di Paolo, M.L., Dalla Via, L., 2021. Promising non-cytotoxic monosubstituted chalcones to target monoamine Oxidase-B. ACS Med. Chem. Lett. 12, 1151–1158. https://doi.org/10.1021/acsmedchemlett.1c00238.
Kassem, A., Abbas, L., Coutinho, O., Opara, S., Najaf, H., Kasperek, D., Pokhrel, K., Li, X., Tiquia-Arashiro, S., 2023. Applications of Fourier transform-infrared spectroscopy in microbial cell biology and environmental microbiology: advances, challenges, and future perspectives. Front. Microbiol. 14.
Kate, A., Sahu, L.K., Pandey, J., Mishra, M., Sharma, P.K., 2022. Green catalysis for chemical transformation: the need for the sustainable development. Curr. Res. Green Sustain. Chem. 5, 100248. https://doi.org/10.1016/j.crgsc.2021.100248.
Kirchon, A., Feng, L., Drake, H.F., Joseph, E.A., Zhou, H.-C., 2018. From fundamentals to applications: a toolbox for robust and multifunctional MOF materials. Chem. Soc. Rev. 47, 8611–8638. https://doi.org/10.1039/C8CS00688A.
Kumawat, T.K., Kumawat, V., Sharma, S., Kandwani, N., Biyani, M., 2021. Applications of EPS in environmental bioremediations. In: Nadda, A.K., Sajna, K.V., Sharma, S. (Eds.), Microbial Exopolysaccharides as Novel and Significant Biomaterials, Springer Series on Polymer and Composite Materials. Springer International Publishing, Cham, pp. 285–302. https://doi.org/10.1007/978-3-030-75289-7_11.
Marmiroli, M., Lepore, G.O., Pagano, L., d'Acapito, F., Gianoncelli, A., Villani, M., Lazzarini, L., White, J.C., Marmiroli, N., 2020. The fate of CdS quantum dots in plants as revealed by extended X-ray absorption fine structure (EXAFS) analysis. Environ. Sci. Nano 7, 1150–1162. https://doi.org/10.1039/C9EN01433K.
Mezgebe, K., Melaku, Y., Mulugeta, E., 2023. Synthesis and pharmacological activities of chalcone and its derivatives bearing N-Heterocyclic scaffolds: a review. ACS Omega. https://doi.org/10.1021/acsomega.3c01035.
Molander, G.A., Cavalcanti, L.N., García-García, C., 2013. Nickel-catalyzed borylation of halides and pseudohalides with tetrahydroxydiboron [B2(OH)4]. J. Org. Chem. 78, 6427–6439. https://doi.org/10.1021/jo401104y.
Momin, S.C., Pradhan, R.B., Nath, J., Lalmuanzeli, R., Kar, A., Mehta, S.K., 2024. Metal sequestration by microcystis extracellular polymers: a promising path to greener water treatment. Environ. Sci. Pollut. Res. 31, 11192–11213. https://doi.org/10.1007/s11356-023-31755-3.
Montargès-Pelletier, E., Chardot, V., Echevarria, G., Michot, L.J., Bauer, A., Morel, J.-L., 2008. Identification of nickel chelators in three hyperaccumulating plants: an X-ray spectroscopic study. Phytochemistry 69, 1695–1709. https://doi.org/10.1016/j.phytochem.2008.02.009.
Mota, R., Flores, C., Tamagnini, P., 2022. Cyanobacterial Extracellular Polymeric Substances (EPS). In: Oliveira, J.M., Radhouani, H., Reis, R.L. (Eds.), Polysaccharides of Microbial Origin. Springer International Publishing, Cham, pp. 139–165. https://doi.org/10.1007/978-3-030-42215-8_11.
Mota, R., Rossi, F., Andrenelli, L., Pereira, S.B., De Philippis, R., Tamagnini, P., 2016. Released polysaccharides (RPS) from cyanothece sp. CCY 0110 as biosorbent for heavy metals bioremediation: interactions between metals and RPS binding sites. Appl. Microbiol. Biotechnol. 100, 7765–7775. https://doi.org/10.1007/s00253-016-7602-9.
Murrieta, M.F., Cornejo, O.M., Rivera, F.F., Nava, J.L., 2024. Electrochemical recovery of inorganic value-added products from wastewater: toward a circular economy model. Curr. Opin. Electrochem. 46, 101498. https://doi.org/10.1016/j.coelec.2024.101498.
Pagnucco, G., Overfield, D., Chamlee, Y., Shuler, C., Kassem, A., Opara, S., Najaf, H., Abbas, L., Coutinho, O., Fortuna, A., Sulaiman, F., Farinas, J., Schittenhelm, R., Catalfano, B., Li, X., Tiquia-Arashiro, S.M., 2023. Metal tolerance and biosorption capacities of bacterial strains isolated from an urban watershed. Front. Microbiol. 14, 1278886. https://doi.org/10.3389/fmicb.2023.1278886.
Pokrovsky, O.S., Pokrovski, G.S., Gélabert, A., Schott, J., Boudou, A., 2005. Speciation of Zn associated with diatoms using X-ray absorption spectroscopy. Environ. Sci. Technol. 39, 4490–4498. https://doi.org/10.1021/es0480419.
Pokrovsky, O.S., Pokrovski, G.S., Shirokova, L.S., Gonzalez, A.G., Emnova, E.E., Feurtet-Mazel, A., 2012. Chemical and structural status of copper associated with oxygenic and anoxygenic phototrophs and heterotrophs: possible evolutionary consequences. Geobiology 10, 130–149. https://doi.org/10.1111/j.1472-4669.2011.00303.x.
Priya, A.K., Gnanasekaran, L., Dutta, K., Rajendran, S., Balakrishnan, D., Soto-Moscoso, M., 2022. Biosorption of heavy metals by microorganisms: evaluation of different underlying mechanisms. Chemosphere 307, 135957. https://doi.org/10.1016/j.chemosphere.2022.135957.
Ramesh, B., Saravanan, A., Senthil Kumar, P., Yaashikaa, P.R., Thamarai, P., Shaji, A., Rangasamy, G., 2023. A review on algae biosorption for the removal of hazardous pollutants from wastewater: limiting factors, prospects and recommendations. Environ. Pollut. 327, 121572. https://doi.org/10.1016/j.envpol.2023.121572.
Ren, X., Feng, M., Mao, M., Long, X., Pan, J., Tang, Y., Zhou, P., Peng, T., Wang, H., Yang, F., 2025. Cyanobacteria for environmental, energy and biomedical application: a review. Environ. Chem. Lett. 23, 491–515. https://doi.org/10.1007/s10311-024-01814-3.
Rossi, F., De Philippis, R., 2016. Exocellular polysaccharides in microalgae and cyanobacteria: chemical features, role and enzymes and genes involved in their biosynthesis. In: Borowitzka, M.A., Beardall, J., Raven, J.A. (Eds.), The Physiology of Microalgae, Developments in Applied Phycology. Springer International Publishing, Cham, pp. 565–590. https://doi.org/10.1007/978-3-319-24945-2_21.
Rossino, G., Robescu, M.S., Licastro, E., Tedesco, C., Martello, I., Maffei, L., Vincenti, G., Bavaro, T., Collina, S., 2022. Biocatalysis: a smart and green tool for the preparation of chiral drugs. Chirality 34, 1403–1418. https://doi.org/10.1002/chir.23498.
Ruffing, A.M., 2011. Engineered cyanobacteria: teaching an old bug new tricks. Bioeng. Bugs 2, 136–149. https://doi.org/10.4161/bbug.2.3.15285.
Salehizadeh, H., Shojaosadati, S.A., 2003. Removal of metal ions from aqueous solution by polysaccharide produced from *Bacillus firmus*. Water Res. 37, 4231–4235. https://doi.org/10.1016/S0043-1354(03)00418-4.
Samoraj, M., Tuhy, Ł., Chojnacka, K., 2019. Valorization of biomass into micronutrient fertilizers. Waste Biomass Valoriz. 10, 925–931. https://doi.org/10.1007/s12649-017-0108-6.
Shilpa, T., Neetha, M., Anilkumar, G., 2021. Recent trends and prospects in the copper-catalysed "on Water" reactions. Adv. Synth. Catal. 363, 1559–1582. https://doi.org/10.1002/adsc.202001407.
VanZile, M.L., Cosper, N.J., Scott, R.A., Giedroc, D.P., 2000. The zinc metalloregulatory protein synechococcus PCC7942 SmtB binds a single zinc ion per monomer with high affinity in a tetrahedral coordination geometry. Biochemistry 39, 11818–11829. https://doi.org/10.1021/bi001140o.
WalyEldeen, A.A., Sabet, S., El-Shorbagy, H.M., Abdelhamid, I.A., Ibrahim, S.A., 2023. Chalcones: promising therapeutic agents targeting key players and signaling pathways regulating the hallmarks of cancer. Chem. Biol. Interact. 369, 110297. https://doi.org/10.1016/j.cbi.2022.110297.
Wu, Z., Fernandez-Lima, F.A., Russell, D.H., 2010. Amino acid influence on copper binding to peptides: cysteine versus arginine. J. Am. Soc. Mass Spectrom. 21, 522–533. https://doi.org/10.1016/j.jasms.2009.12.020.
Yadav, A.P.S., Dwivedi, V., Kumar, S., Kushwaha, A., Goswami, L., Reddy, B.S., 2021. Cyanobacterial extracellular polymeric substances for heavy metal removal: a mini review. J. Compos. Sci. 5, 1. https://doi.org/10.3390/jcs5010001.
Zanetti, R., Zecchin, S., Colombo, M., Borgonovo, G., Mazzini, S., Scaglioni, L., Facchetti, G., Gandolfi, R., Rimoldi, I., Cavalca, L., 2022. Ni2+ and Cu2+ biosorption by EPS-producing Serratia plymuthica strains and potential bio-catalysis of the organo–metal complexes. Water 14, 3410. https://doi.org/10.3390/w14213410.
Zhang, L., Wei, Z., Meng, M., Ung, G., He, J., 2020. Do polymer ligands block the catalysis of metal nanoparticles? Unexpected importance of binding motifs in improving catalytic activity. J. Mater. Chem. A 8, 15900–15908. https://doi.org/10.1039/D0TA03906C.